Mon. Not. R. Astron. Soc. **000**, 000–000 (0000) Printed 28 June 2011 (MN LATEX style file v1.4)

Radiative transfer in disc galaxies I – A comparison of four methods to solve the transfer equation in plane-parallel geometry

Maarten Baes⋆ and Herwig Dejonghe
Sterrenkundig Observatorium Universiteit Gent, Krijgslaan 281 S9, B-9000 Gent, Belgium, maarten.baes@rug.ac.be

28 June 2011

ABSTRACT
Accurate photometric and kinematic modelling of disc galaxies requires the inclusion of radiative transfer models. Due to the complexity of the radiative transfer equation (RTE), sophisticated techniques are required. Various techniques have been employed for the attenuation in disc galaxies, but a quantitative comparison of them is difficult, because of the differing assumptions, approximations and accuracy requirements which are adopted in the literature. In this paper, we present an unbiased comparison of four methods to solve the RTE, in terms of accuracy, efficiency and flexibility. We apply them all on one problem that can serve as a first approximation of large portions of disc galaxies: a one-dimensional plane-parallel geometry, with both absorption and multiple scattering taken into account, with an arbitrary vertical distributions of stars and dust and an arbitrary angular redistribution of the scattering. We find that the spherical harmonics method is by far the most efficient way to solve the RTE, whereas both Monte Carlo simulations and the iteration method, which are straightforward to extend to more complex geometries, have a cost which is about 170 times larger.

Key words: radiative transfer – methods: numerical

1 INTRODUCTION

In order to study the structure of galaxies, it is necessary to obtain their intrinsic three-dimensional light distribution, i.e. to deproject their two-dimensional image. This deprojection is complicated by the effects of interstellar dust, which change the radiation field on its way through the galaxy by absorption, emission and scattering. The amount of interstellar dust present in disc galaxies has been the subject of debate for the last few years. The most widely supported idea is that spiral galaxies are moderately optically thick in their central regions (a face-on optical depth of order unity in the V band), and optically thin in the outer regions. This idea is supported by statistical studies (Giovanelli et al. 1994, Boselli & Gavazzi 1994, Buat & Burgarella 1998), studies of the extinction of galaxies in overlapping pairs (White & Keel 1992, Berlind et al. 1997, Rönnback & Shaver 1997, Pizagno & Rix 1998, White et al. 2000), and detailed modelling of the extinction in individual galaxies (Jansen et al. 1994, Ohta & Kodaira 1995, Xilouris et al. 1997, 1998, 1999, Kuchinski et al. 1998). However, there is still no consensus, and other authors claim that spiral galaxies are optically thick all over their disc (Valentijn 1990, 1994, Burnstein et al. 1991, James & Puxley 1993, Peletier et al. 1995). Moreover other arguments complicate the discussion: it is a gross simplification to talk about *the* opacity of spiral galaxies, because there can be a large difference in opacity between arm and interarm regions (White et al. 2000). For a detailed overview of the opacity of disc galaxies we refer to Davies & Burnstein (1995) and Kuchinski et al. (1998).

Many authors have demonstrated that dust attenuation (i.e. the combined effect of absorption and scattering) has considerable effects on photometric properties such as magnitudes, colors and scalelengths (Witt et al. 1992, Byun et al. 1994, Corradi et al. 1996). These effects are of a complicated nature, and are not simply proportional to the optical depth of the galaxy. Also kinematic studies can be complicated by dust attenuation because the projected kinematics will be biased towards the motions of stars on the near side of the line-of-sight (Bosma et al. 1992, Matthews & Wood 2000, Baes & Dejonghe 2001a). Both photometric and kinematic studies of disc galaxies hence require sophisticated deprojection techniques which take dust attenuation into account. The only means to do this properly is by constructing radiative transfer models.

The radiative transfer problem is a well-defined prob-

⋆ Research Assistent of the Fund of Scientific Research – Flanders (Belgium)

lem. It is described by the radiative transfer equation (RTE), which requires as input a precise knowledge of the optical properties of the dust grains, the opacity (the total amount and the spatial distribution of the dust) and the emissivity (the spatial and energy distribution of the stars). If a convenient algorithm is found to solve the equation, the output is the projected image on the sky, or the surface brightness. But usually the problem is the reverse. Given the observed image on the plane of the sky, can we recover the three-dimensional distribution of stars and dust ? The most straightforward way to solve this problem is to construct a large set of models with various parameters, solve the transfer equation for each of these models, and then determine the parameters such that the obtained solution fits the observations. It is clear that efficient algorithms to solve the RTE are necessary.

Unfortunately, the RTE is a fairly complicated equation, and it is not straightforward to solve it, unless some simplifying assumptions are made. The most widely adopted way to simplify the RTE is an approximation or downright neglect of the scattering by dust grains (Guiderdoni & Rocca-Volmerange 1987, Disney et al. 1989, Calzetti et al. 1994, Ohta & Kodaira 1995). Nevertheless many efforts have been made to develop methods to solve the RTE exactly. Four of the methods that have been explored are

- *the spherical harmonics method*, where all terms in the RTE are expanded into a series of spherical harmonics, such that the RTE is replaced by a set of ordinary differential equations.
- *the discretization method*, a technique borrowed from the stellar atmospheres theory. In this method integrals are replaced by sums and the differentials by finite differences, resulting in a set of vector equations which can be solved iteratively.
- *the iteration method*, where intensity is expanded in a series of partial intensities. Each of the partial intensities obeys its own RTE, which can be solved iteratively.
- *Monte Carlo simulations*, where the transfer of photons through the galaxy is investigated by examining the individual paths of a large number of photons.

Each of these methods will have its advantages and disadvantages. On the one hand the different approaches have different physical backgrounds, and the selection of a certain algorithm can be useful to gain physical insight into the problem. For example, the spherical harmonics method gives direct access to the moments of the radiation field, whereas the iteration method yields direct information about the importance of multiple scattering. On the other hand, computational and practical considerations can be motives to prefer one method above another. However, these considerations are often based on general truths without a quantification. For example, it is generally accepted that Monte Carlo methods are costly, but how costly in respect with other methods ?

It is important to be able to estimate how a certain solution method scores in terms of accuracy, efficiency and flexibility. According to one's specific interest (e.g. providing a tool for statistical studies of attenuation, or constructing detailed radiative transfer models for individual galaxies), one of these properties may be more important than another. Knowing the relative performance of the different methods then allows to select the most suitable candidate for the problem.

The aim of this paper is to present an unbiased comparison of the four methods considered. All of them have already been applied to construct radiative transfer models in order to investigate the attenuation in disc galaxies (references will be given). However, the assumptions concerning the geometry and the dust properties made by the various authors often differ significantly. This makes a comparison of the various adopted methods in the literature in terms of accuracy, efficiency and flexibility next to impossible. Therefore we adapt them such that they can be used to solve the same radiative transfer problem. We restrict ourselves to a one-dimensional plane-parallel geometry, however with absorption and multiple scattering properly accounted for. Moreover, all of these models allow an arbitrary vertical distribution of stars and dust, and an arbitrary angular redistribution function (ARF), such that they can serve as a first approximation to model large portions of galactic discs.

In Section 2 we discuss the radiative transfer problem and present a disc galaxy model to illustrate the solution techniques, which are presented in the next four sections. In Section 3 the RTE is solved by an expansion in spherical harmonics, in Section 4 we describe the discretization technique, in Section 5 the RTE is solved by an iterative method, and in Section 6 a Monte Carlo simulation is used. In Section 7 we compare the different techniques in terms of accuracy and numerical efficiency, and we discuss them in the light of their use to construct detailed models for disc galaxies. Section 8 sums up.

2 THE RADIATIVE TRANSFER PROBLEM

2.1 The RTE in plane-parallel geometry

In plane-parallel geometry, there are only two independent variables necessary to determine a position and a direction in the galaxy: the depth z, and μ, the cosine of the angle between that direction and the face-on direction (plane-parallel geometry implies an azimuthal symmetry around the face-on direction $\mu = 1$). The general form of the transfer equation in plane-parallel geometry can be written as (in this paper we omit all explicit reference to the wavelength dependences)

$$\mu \frac{\partial I}{\partial z}(z,\mu) = -\kappa(z) I(z,\mu) + \eta_*(z) + \frac{1}{2}\omega\kappa(z) \int_{-1}^{1} I(z,\mu')\Psi(\mu,\mu')\mathrm{d}\mu'. \quad (1)$$

Here $I(z,\mu)$ is the specific intensity of the radiation, $\kappa(z)$ is the dust opacity, $\eta_*(z)$ is the stellar emissivity, ω the dust albedo and $\Psi(\mu,\mu')$ is the ARF. The last term in equation (1) represents the scattering term, i.e. the net amount of photons which are scattered off dust grains into the direction μ from all other directions μ' at z (see Appendix A). We assume that the scattering is coherent, i.e. there is no energy redistribution of the scattered light. The thermal emission of the absorbed light by the dust grains is neglected, because this occurs at far-infrared wavelengths, whereas we will focus on shorter wavelengths. Furthermore we assume that the dust grains have the same properties over the galaxy. This

means that the albedo and the redistribution function are independent of position, and that both the emissivity and the opacity are separable functions of position and wavelength.

We replace the height z above the galactic plane by the optical depth τ, defined as

$$\tau(z) = \int_z^\infty \kappa(z')\mathrm{d}z', \tag{2}$$

and the RTE then becomes

$$\mu \frac{\partial I}{\partial \tau}(\tau,\mu) = I(\tau,\mu) - S_*(\tau) - \frac{\omega}{2}\int_{-1}^{1} I(\tau,\mu')\Psi(\mu,\mu')\mathrm{d}\mu', \tag{3}$$

where $S_*(\tau) = \eta_*(\tau)/\kappa(\tau)$ is the stellar source function. This equation is to be solved for $0 \leqslant \tau \leqslant \tau_0$, the total optical depth of the slab,

$$\tau_0 = \int_{-\infty}^{\infty} \kappa(z)\mathrm{d}z. \tag{4}$$

The boundary conditions for our radiative transfer problem are

$$I(0,-\mu) = I(\tau_0,\mu) = 0 \qquad \text{for } \mu > 0, \tag{5}$$

which means that there is no incident radiation on either side of the galaxy. The RTE (3), together with the boundary conditions (5) allow us to calculate the radiation field at any position and into any direction in the galaxy. In the first place however, we are interested in the radiation field $I(0,\mu)$ that leaves the galaxy at $\tau = 0$ into a certain direction μ, and more precisely in the fraction of this intensity that is attenuated. Because the RTE is a linear equation, this fraction will be independent of the total amount of stellar emission. We can thus choose the normalization of the stellar emissivity (or the source function) arbitrarily. We take

$$\int_{-\infty}^{\infty} \eta_*(z)\,\mathrm{d}z = \int_0^{\tau_0} S_*(\tau)\,\mathrm{d}\tau = 1, \tag{6}$$

which means that the intensity that leaves the galaxy in the absence of dust in the face-on direction equals 1. In another direction μ, the dust-free intensity is then simply $1/\mu$ and the attenuation (in magnitudes) is

$$A(\mu) = -2.5\log\left[\mu\, I(0,\mu)\right]. \tag{7}$$

2.2 A disc galaxy model

In order to solve the problem we still need to characterize the parameters and functions that appear in (1), i.e. the optical properties of the dust and the spatial distribution of stars and dust have to be specified. Because the present paper focuses on the comparison of different methods to solve the RTE rather than on an investigation of the impact of dust attenuation on disc galaxies, we restrict ourselves here to a single galaxy model to illustrate our results. For a thorough study of the attenuation curve as a function of various parameters determining the distribution of stars and dust, we refer to the second paper in this series (Baes & Dejonghe 2001b).

The vertical distribution of stars in disc galaxies is still a matter of debate. Stars were first believed to be isothermally distributed in the z-direction (van der Kruit & Searle 1981), and later on an exponential behavior was proposed (Wainscoat et al. 1989). Nowadays it is believed that the true distribution lies in between these two profiles (Pohlen et al. 2000, Schwarzkopf & Dettmar 2000). We adopt an exponential profile,

$$\eta_*(z) = \frac{1}{2h}\,\mathrm{e}^{-|z|/h}, \tag{8}$$

where h is the scaleheight, which satisfies the normalization condition (6). For the dust distribution we also assume an exponential distribution. In a normal disc galaxy, the interstellar matter will sink down to the central plane and form an obscuring layer which is narrower than the stellar layer. Detailed radiative transfer models of edge-on galaxies indicate that the scaleheight of the dust is about half of the stellar one (Xilouris et al. 1999). As opacity function we then obtain

$$\kappa(z) = \frac{\tau_0}{h}\,\mathrm{e}^{-2|z|/h}. \tag{9}$$

The normalization of (9) is such that (4) is satisfied. For the total optical depth we adopt a moderate value $\tau_V = 1$, which seems to be appropriate for disc galaxies, as we argued in the introduction.

For $\Psi(\mu,\mu')$ we adopt the Henyey-Greenstein ARF (see Appendix A), appropriate to describe anisotropic scattering. It is a one-parameter function with a (wavelength dependent) parameter g, which is called the asymmetry parameter and is the average of the cosine of the scattering angle. Values for the optical properties of the dust grains (the wavelength dependence of the opacity κ, the albedo ω and the asymmetry parameter g) are those calculated by Maccioni & Perinotto (1994) and displayed in Di Bartolomeo et al. (1995). The adopted values of the U, B, V, R and I bands are tabulated in Table 1.

Table 1. The adopted values for the optical properties of the dust grains. Tabulated are the optical depth τ relative to the V-band value, the scattering albedo ω and the asymmetry parameter g.

band	$\lambda\,(\mu\mathrm{m})$	τ	ω	g
U	360	1.60	0.57	0.49
B	440	1.32	0.57	0.48
V	550	1.00	0.57	0.44
R	700	0.73	0.54	0.37
I	850	0.47	0.51	0.31

We wish to stress again that this galaxy model is only illustrative, and that the methods discussed in this paper are applicable to *any* galaxy model of the kind we consider here, i.e. with arbitrary vertical distribution of stars and dust and with arbitrary ARF.

3 THE SPHERICAL HARMONICS METHOD

One of the most popular techniques to solve the radiative transfer equation is a method which uses an expansion in spherical harmonics. Many papers have been written which describe this method in detail, e.g. Davison (1957), Flannery et al. (1980), Roberge (1983), Di Bartolomeo et al. (1995). Our approach is based on Roberge (1983), whose method can account for any vertical distribution of stars and dust, and uses the adaptations of Di Bartolomeo et al. (1995) in order to make the matrix in the eigenvalue problem symmetric.

In plane-parallel symmetry, spherical harmonics reduce to Legendre polynomials, and we expand the intensity and the redistribution function in a series of Legendre polynomials,

$$I(\tau,\mu) = \sum_{l=0}^{\infty} (2l+1) f_l(\tau) P_l(\mu) \tag{10}$$

$$\Psi(\mu,\mu') = \sum_{l=0}^{\infty} (2l+1) \sigma_l P_l(\mu) P_l(\mu'). \tag{11}$$

The coefficients $f_l(\tau)$ are unknown functions, whereas the coefficients σ_l are known. For example, in the case of Henyey-Greenstein scattering, $\sigma_l = g^l$, with g the asymmetry parameter (Appendix A). Inserting the expansions (10) and (11) in (3), and using the recurrence relations for Legendre polynomials, we find

$$\sum_{l=0}^{\infty} \Big[l f'_{l-1}(\tau) + (l+1) f'_{l+1}(\tau) - h_l f_l(\tau) \Big] P_l(\mu) = -S_*(\tau), \tag{12}$$

where we set $h_l = (2l+1)(1-\omega\sigma_l)$. Defining the functions ψ_l and g_l as

$$\psi_l(\tau) = \sqrt{h_l} f_l(\tau) \tag{13}$$

$$g_l(\tau) = -\frac{S_*(\tau)}{\sqrt{h_0}} \delta_{l,0}, \tag{14}$$

we find an infinite set of linear first-order differential equations

$$\frac{l}{\sqrt{h_l h_{l-1}}} \psi'_{l-1}(\tau) + \frac{l+1}{\sqrt{h_{l+1} h_l}} \psi'_{l+1}(\tau) = \psi_l(\tau) + g_l(\tau). \tag{15}$$

We adopt the so-called P_L approximation (consists in assuming $\psi_l(\tau) = 0$ for $l > L$, for a certain value of L, L odd) in order to turn this infinite set into a finite one, which we can write as a vector equation

$$\mathcal{A}\boldsymbol{\psi}'(\tau) = \boldsymbol{\psi}(\tau) + \boldsymbol{g}(\tau). \tag{16}$$

The RTE is thus reduced to a set of ordinary differential equations, for which the system matrix $\mathcal{A}$ is a non-singular, symmetric, tridiagonal matrix with fixed coefficients. Such a problem is best solved by diagonalization of the matrix, i.e. an eigenvalue problem. The procedure to obtain the expressions for $\psi_l(\tau)$, are nicely described in Roberge (1983).

We note in particular that for the P_L solution, the two boundary conditions (5) can only be satisfied for $(L+1)/2$ directions μ_i, which are the positive zeros of the Legendre polynomial of order $L+1$. The intensity

$$I(\tau,\mu) = \sum_{l=0}^{L} \frac{2l+1}{\sqrt{h_l}} \psi_l(\tau) P_l(\mu). \tag{17}$$

at other directions can be obtained by a cubic spline interpolation. In general we found that the P_L solution converges very fast, and that the boundary conditions were met when $L \gtrsim 15$, which we adopted in our calculations. This value is slightly larger than that used by Di Bartolomeo et al. (1995).

4 THE DISCRETIZATION METHOD

One of the first major efforts to investigate the effects of absorption and multiple scattering in disc galaxies, is the paper by Bruzual et al. (1988). They solve the RTE for a galaxy model consisting of a homogeneous mixture of stars and dust. Their technique is based on a discretization of the RTE on a fixed mesh of points, and difference equations replace the differential equations. We extend the technique of Bruzual et al. (1988) such that it can account for any vertical distribution of stars and dust, i.e. any source function $S_*(\tau)$. As we will discuss in section 4.2, we will have to make a distinction between source functions that remain finite everywhere and source functions that diverge in places.

4.1 Finite source functions

If the source function $S_*(\tau)$ remains finite for all values of τ, we can easily generalize the procedure of Bruzual et al. (1988). Starting from the transfer equation (3) we introduce the even and odd fields

$$u(\tau,\mu) = \tfrac{1}{2}\left[I(\tau,\mu) + I(\tau,-\mu)\right] \tag{18}$$

$$v(\tau,\mu) = \tfrac{1}{2}\left[I(\tau,\mu) - I(\tau,-\mu)\right]. \tag{19}$$

The transfer equation can then be written as

$$\mu \frac{\partial u}{\partial \tau}(\tau,\mu) = v(\tau,\mu) - \omega \int_0^1 v(\tau,\mu') \Psi^o(\mu,\mu') \mathrm{d}\mu' \tag{20}$$

$$\mu \frac{\partial v}{\partial \tau}(\tau,\mu) = u(\tau,\mu) - S_*(\tau) - \omega \int_0^1 u(\tau,\mu') \Psi^e(\mu,\mu') \mathrm{d}\mu', \tag{21}$$

where

$$\Psi^e(\mu,\mu') = \tfrac{1}{2}\left[\Psi(\mu,\mu') + \Psi(\mu,-\mu')\right] \tag{22}$$

$$\Psi^o(\mu,\mu') = \tfrac{1}{2}\left[\Psi(\mu,\mu') - \Psi(\mu,-\mu')\right]. \tag{23}$$

The new boundary conditions are

$$u(0,\mu) = v(0,\mu) \tag{24}$$

$$u(\tau_0,\mu) = -v(\tau_0,\mu). \tag{25}$$

These equations are analogous to the ones Bruzual et al. (1988) use for their homogeneous slab, with the exception that the constant source function for the homogeneous slab is replaced by a non-constant, but finite source function $S_*(\tau)$. A similar discretization procedure can be followed. We introduce a grid of $N+1$ mesh points τ_i, uniformly spaced in optical depth space. In between these points we introduce a second grid, denoted by half-integer numbers $\tau_{i+1/2}$. A derivative evaluated in a half-integer grid point $\tau_{i+1/2}$ becomes a difference evaluated in the nearest integer mesh points τ_i and τ_{i+1}, and analogous for the integer mesh points. At the boundaries τ_0 and τ_N the derivatives are expressed by means of the boundary conditions. The integrals over μ are approximated by M-point Gauss-Legendre quadrature, and we hence introduce a mesh of M points μ_j, being the roots of the Mth order Legendre polynomial. The RTEs are then replaced by a set of linear vector equations, where the $(2N+1)M$ unknowns are the even and odd fields $u_{i,j}$ and $v_{i+1/2,j}$ evaluated at the integer and half-integer mesh points respectively. These equations are solved recursively using (a simplification of) the elimination scheme of Milkey et al. (1975).

Optimal values for M and N are hard to determine. On the one hand these values should not be too high, because of computational limitations. Indeed, the elimination scheme consists of two loops, and every step in the first loop

consists of 2 matrix inversions, where the order of the matrices is M, the number of angle quadrature points. This means that totally $2N+1$ matrices of order M need to be inverted, which is a numerically costly process. Moreover, the memory requirement is high, because the $2N+1$ matrices calculated in the first loop need to be stored, for use in the second loop. On the other hand, the values for M and N should not be taken too low, such that the approximation of differentials by differences and integrals by quadrature sums is acceptable. Typically $M = 10$, while typical values for N are dependent on the total optical depth τ_0 and should be chosen such that $\Delta\tau$ never exceeds 0.01. For our galaxy model this meant $N \gtrsim 100$.

4.2 Diverging source functions

The above procedure cannot be used anymore when the source function diverges at the boundaries $\tau = 0$ and/or $\tau = \tau_0$, because the source function needs to be evaluated in these end points. Such source functions are realistic, because they correspond to all distributions where the dust distribution is narrower than the stellar distribution, which is observed in most galaxies. In particular, the galaxy model described in Section 2.2 has a diverging source function.

One obvious solution would be to apply a cutoff, but the method then becomes very dependent on the actual position of the cutoff. Moreover such a solution is inaccurate, because it involves a lot of matrix inversions, and these are difficult operations if the matrices contain elements of very different magnitudes.

If the source function diverges, we don't use the optical depth coordinates, but we define a similar independent variable ξ,

$$\xi(z) = \int_z^\infty \eta_*(z')\,\mathrm{d}z', \tag{26}$$

which assumes values between 0 and 1, because of the normalization of the emissivity (6). The RTE (1) becomes

$$\mu\,\frac{\partial I}{\partial \xi}(\xi,\mu) = R_*(\xi)\,I(\xi,\mu) - 1 - \frac{1}{2}\omega R_*(\xi)\int_{-1}^{1} I(\xi,\mu')\Psi(\mu,\mu')\mathrm{d}\mu', \tag{27}$$

where R_* is the reciprocal of the stellar source function,

$$R_*(\xi) = \frac{1}{S_*(\xi)} = \frac{\kappa(\xi)}{\eta_*(\xi)}. \tag{28}$$

Starting from this form of the RTE, we can repeat the discretization procedure from the previous paragraph, i.e. we construct a uniform mesh ξ_i and an intermediate mesh $\xi_{i+1/2}$ for the finite differences, and a mesh μ_j for the Legendre-Gauss quadrature, and we obtain a set of vector equations for the unknowns $u_{i,j}$ and $v_{i+1/2,j}$, which are solved by the elimination scheme of Milkey et al. (1975).

The arguments leading to the choice of N and M are the same as in the previous paragraph.

5 ITERATION METHODS

5.1 The intensity as a series

In a very early paper on scattering, Henyey (1937) shows that the RTE (3) can be solved iteratively by writing the intensity as a summation of partial intensities I_n, which represent the radiation field consisting of photons that have been scattered exactly n times. This technique has been adopted by van de Hulst & de Jong (1969) and Xu & Helou (1996) to solve the RTE in plane-parallel geometry. Specifically in our case, we write the intensity as

$$I(\tau,\mu) = \sum_{n=0}^{\infty} I_n(\tau,\mu), \tag{29}$$

The nth partial intensity satisfies the RTE

$$\mu\,\frac{\partial I_n}{\partial \tau}(\tau,\mu) = I_n(\tau,\mu) - S_n(\tau,\mu), \tag{30}$$

where

$$S_0(\tau,\mu) = S_*(\tau) \tag{31}$$

$$S_n(\tau,\mu) = \frac{\omega}{2}\int_{-1}^{1} I_{n-1}(\tau,\mu')\Psi(\mu,\mu')\mathrm{d}\mu', \tag{32}$$

and is subject to the boundary conditions

$$I_n(0,-\mu) = I_n(\tau_0,\mu) = 0 \qquad \text{for } \mu > 0. \tag{33}$$

The solution of (30) can be directly written

$$I_n(\tau,\mu) = \frac{1}{\mu}\int_\tau^{\tau_0} S_n(\tau',\mu)\,\exp\left(\frac{\tau-\tau'}{\mu}\right)\mathrm{d}\tau' \tag{34}$$

$$I_n(\tau,-\mu) = \frac{1}{\mu}\int_0^{\tau} S_n(\tau',\mu)\,\exp\left(\frac{\tau'-\tau}{\mu}\right)\mathrm{d}\tau'. \tag{35}$$

We calculated the partial intensities and source functions on a mesh of size L in optical depth and size M in angle. Because the integration over the angle in (32) always has the same integration domain, we chose the M angle points as the abscissae for an M-point Gauss-Legendre quadrature. For the calculation of the I_n, the integration along the path has variable boundaries, and hence a simple quadrature would yield bad results near the edges of the mesh. Instead, we used a uniform mesh of optical depth points, and for each fixed angle μ_j, we constructed a cubic spline approximation to $S_n(\tau,\mu_j)$, and performed the integration using this function. Typical values for L and M are 40 and 10 respectively.

The number of terms necessary in the summation (29) in order to obtain an accurate result depends on the wavelength, because the nth term in the expansion is proportional to the nth power of the albedo ω^n. Xu & Helou (1996) used 20 terms for their sandwich model; we find that in general, about 10 terms are sufficient. For our one-dimensional plane-parallel geometry this number of integrations is still manageable. However, if the method is extended to more complicated geometries, more dimensions will be added, and calculation of such a high number of terms becomes very time-consuming, such that adaptations of the method are desirable.

5.2 The intensity as a geometric series

A simplification of the iteration method was introduced by Kylafis & Bahcall (1987). They use the approximation that the amount of photons that are scattered exactly $n+1$ times

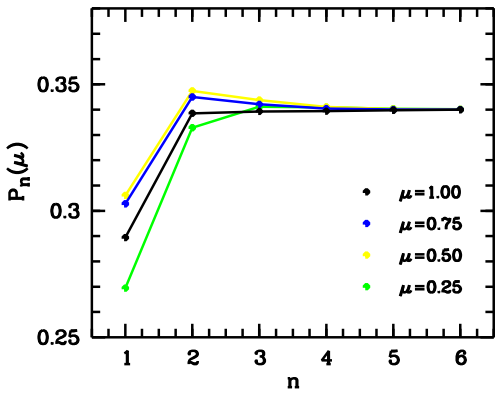

Figure 1. The ratio $P_n(\mu) = I_n(0,\mu)/I_{n-1}(0,\mu)$ at the V band of two consecutive terms in the series (29), as a function of n. It is shown for four different inclination angles, for the model described in Section 2.2.

to the amount of photons scattered exactly n times, is constant, i.e.

$$\frac{I_{n+1}(\tau,\mu)}{I_n(\tau,\mu)} = \frac{I_n(\tau,\mu)}{I_{n-1}(\tau,\mu)} \qquad \text{for all } n. \tag{36}$$

If this approximation holds, only two terms in the sum (29) need to be calculated, because it can be written as a geometric series

$$I(\tau,\mu) = I_0(\tau,\mu)\sum_{j=0}^{\infty}\left[\frac{I_1(\tau,\mu)}{I_0(\tau,\mu)}\right]^j. \tag{37}$$

To test the accuracy of the approximation (36), we calculated several terms in the sum (29) for our galaxy model. The results are shown in Figure 1, where we plot the ratio $P_n(\mu) = I_n(0,\mu)/I_{n-1}(0,\mu)$ as a function of n, for four different values of μ. It is clear that $P_n(\mu)$ is indeed constant for $n \gtrsim 3$, and that this constant is independent of the angle μ. For the first values of n however, the condition (36) is clearly not satisfied. Therefore we adapt the strategy of Kylafis & Bahcall (1987), and we assume that the condition (36) is valid for $n > N$. The intensity can then be written as

$$I(\tau,\mu) = I_0(\tau,\mu) + I_1(\tau,\mu) + \cdots + I_{N-1}(\tau,\mu)\sum_{j=0}^{\infty}\left[\frac{I_N(\tau,\mu)}{I_{N-1}(\tau,\mu)}\right]^j. \tag{38}$$

The parameter N thus determines the last of the partial intensities that needs to be calculated explicitly. We find that already for $N = 2$ the results are correct with less than a one-percent error. The number of integrations that then has to be performed for the solution of the RTE is $3LM$.

6 MONTE CARLO SIMULATION

The last method we considered to solve the RTE is a Monte Carlo simulation, which is probably the most widely adopted method for radiative transfer problems. The principles of this method are described in detail by Cashwell & Everett (1959), Mattila (1970), Witt (1977), Yusef-Zadeh et al. (1984) and Bianchi et al. (1996).

6.1 The principles

The Monte Carlo method basically follows the individual path of a very large number N of photons through the galaxy. At each moment, the fate of a photon on its path is determined by a number of quantities such as the free path length between two interactions, the nature of the interaction (scattering or absorption) and the direction change during a scattering event. Each of these quantities can be described by a random variable, taken from a particular probability density $p(x)\mathrm{d}x$.

More specifically, in plane-parallel geometry a photon is characterized by two variables: the position (or equivalently the optical depth τ) and the direction μ. To start, the initial position τ_1 and direction μ_1 are generated randomly as

$$X_1 = \int_0^{\tau_1} S_*(x)\,\mathrm{d}x \tag{39}$$

$$X_2 = \int_{-1}^{\mu_1} \frac{\mathrm{d}x}{2} \quad \text{or} \quad \mu_1 = 2X_2 - 1, \tag{40}$$

where X_1 and X_2 are uniform deviates. Next we generate a random free path length ℓ (also in optical depth units) by setting

$$X_3 = \int_0^{\ell} \mathrm{e}^{-x}\mathrm{d}x \quad \text{or} \quad \ell = -\ln(1-X_3) \tag{41}$$

This randomly determined path length is to be compared with the maximal free path length L of the photon in consideration,

$$L = \begin{cases} \dfrac{\tau_1}{\mu_1} & \text{if } \mu_1 > 0 \\ -\dfrac{\tau_0 - \tau_1}{\mu_1} & \text{if } \mu_1 < 0. \end{cases} \tag{42}$$

If $\ell > L$, the photon will leave the galaxy, and its direction μ_1 is recorded. If $\ell < L$, the photon will interact with a dust grain. The nature of this interaction can be determined by chosing a uniform deviate X_4 and setting

$$\text{interaction} = \begin{cases} \text{scattering} & \text{if } X_4 < \omega \\ \text{absorption} & \text{if } X_4 > \omega. \end{cases} \tag{43}$$

If the interaction is an absorption, the photon disappears and will not contribute to the final intensity. If the interaction is a scattering, the photon will have a new position and a new direction. Given the free path length ℓ and the original position τ_1 and direction μ_1, the new position of the photon is

$$\tau_2 = \tau_1 - \mu_1\ell, \tag{44}$$

whereas the new direction μ_2 is determined by the uniform deviate

$$X_5 = \frac{1}{2}\int_0^{\mu_2} \Psi(\mu_1, x)\,\mathrm{d}x. \tag{45}$$

This procedure can now be repeated until the photon is either absorbed or leaves the galaxy. In the latter case it will contribute to the observed intensity and its direction must be recorded. After a sufficiently large number of such experiments, an M-binned histogram of the emerging angular distribution can be constructed. Due to the planar symmetry of our galaxy models, photons leaving the galaxy at the back side can be added to those leaving at the front side. The ratio of the number of photons to the number of photons

that would be in the bin if there were no dust attenuation (i.e. the distribution of the initial directions), then yields the attenuation in that bin. The final attenuation curve $A(\mu)$ is determined by fitting a smooth curve to these results.

6.2 Optimizing the routine

There are two simple ways in which the above described routine can be optimized, i.e. adapted such that better statistics can be obtained with less photons.

The first adaptation is to avoid that photons disappear from the radiation field by absorption. This can be done by assigning a weight to each photon. At each interaction the probability that the photon will be scattered is ω, whereas the probability for absorption is $1-\omega$. Instead of simulating absorption as described above, we let the photon scatter and we reduce its weight by a factor ω. This way, no photons disappear from the radiation field, and each photon will eventually leave the galaxy. At that point, both direction and weight are recorded. The final histogram is obtained by counting the number of photons in each bin, weighted by their individual weight.

A second adaptation is the concept of forced first scattering, by which each photon is forced to be scattered at least once before it leaves the galaxy. Given the initial maximal free path length $L(\tau,\mu)$ of the photon, the probability that the photon leaves the galaxy is $\exp(-L)$. When the total optical depth of the galaxy is low, many photons leave the galaxy without interaction, such that a large number of photons is necessary to obtain reliable statistics of the scattered radiation. Hence, instead of allowing that a photon can escape from the galaxy, we split it. A fraction with weight $w=\exp(-L)$ leaves the galaxy and will be classified. The other fraction with weight $w=\omega[1-\exp(-L)]$ is forced to scatter before it leaves the galaxy. Therefore a free path length ℓ has to be generated such that $\ell < L$. This can be done by replacing (41) with

$$X_3 = \int_0^\ell \mathrm{e}^{-x}\mathrm{d}x \Big/ \int_0^L \mathrm{e}^{-x}\mathrm{d}x \quad \text{or} \quad \ell = -\ln\left[1-X_3\left(1-\mathrm{e}^{-L}\right)\right]. \quad (46)$$

After this forced first scattering, the following scatterings are as described above.

These two concepts reduce the number of photons, necessary to obtain reliable statistics, significantly. Typical values of N and M we use in our calculations are $N=10^5$ and $M=100$, such that the mean number of photons in each bin is around 1000.

7 DISCUSSION OF THE ADOPTED TECHNIQUES

7.1 Comparison of the numerical results

Because we have at our disposal four different methods to solve the RTE, it is straightforward to check the correctness of the individual methods by comparing their results. In Figure 2 we plot the V band attenuation for the model described in Section 2.2, for the four methods considered. We can obviously conclude that the four modelling procedures are in complete agreement with each other.

Table 2. A check on the accuracy of the four adopted methods of solving the RTE. We computed the attenuation $A(\mu)$ of the model described in Section 2.2, for four angles and for the five bands U, B, V, R and I. The four results correspond to the spherical harmonics method (*sh*), the discretization method (*di*), the iteration method (*it*) and the Monte Carlo simulation (*mc*).

	μ	0.25	0.50	0.75	1.00
U	sh	1.113	0.617	0.356	0.209
	di	1.113	0.617	0.355	0.209
	it	1.119	0.617	0.354	0.208
	mc	1.108	0.616	0.360	0.213
B	sh	1.010	0.520	0.278	0.149
	di	1.010	0.520	0.277	0.148
	it	1.014	0.519	0.276	0.148
	mc	1.003	0.524	0.277	0.129
V	sh	0.865	0.398	0.187	0.081
	di	0.866	0.398	0.187	0.081
	it	0.867	0.397	0.186	0.081
	mc	0.851	0.402	0.188	0.078
R	sh	0.721	0.299	0.123	0.038
	di	0.721	0.298	0.123	0.037
	it	0.722	0.298	0.123	0.038
	mc	0.710	0.300	0.127	0.029
I	sh	0.537	0.197	0.068	0.007
	di	0.538	0.196	0.067	0.006
	it	0.538	0.196	0.067	0.007
	mc	0.533	0.195	0.070	0.007

However, as already mentioned, the modelling techniques do not reveal the solution at any direction μ. The spherical harmonics method only yields A for the $(L+1)/2$ positive zeros of the Legendre polynomial of order $L+1$. The discretization and iteration methods yield A at the abscissae of the adopted quadrature formulae. The Monte Carlo method actually yields a histogram of the attenuation in each of the bins into which the interval of possible μ-values is divided. In order to find the attenuation in a randomly chosen direction μ, we use a spline interpolant for the first three methods, and a fitting polynomial for the Monte Carlo method. In Table 2 we tabulate the attenuation curve $A(\mu)$, calculated by each of the four methods, for four inclination angles μ. This table shows that the differences between the different solutions is always of the order $\Delta A \approx 0.01$ mag. Figure 2 and Table 2 prove that the four methods are accurate and consistent.

In principle, we could also check the correctness of the methods by comparing our results with those obtained by other teams, who adopted similar techniques. Such a comparative analysis is conducted by Di Bartolomeo et al. (1995), who compared their results for a homogeneous slab with those of Guiderdoni & Rocca-Volmerange (1987), Kylafis & Bahcall (1987), Bruzual et al. (1988), Witt et al. (1992), Byun et al. (1994) and Calzetti et al. (1994). The discrepancies between the extinction curves are significant (e.g. ΔA_U up to 0.3 mag for τ_V as small as 0.5), and it is important to investigate why this is so. Are they due to the adopted solution technique or to other causes ? Generally, the discrepancies can be the result of differences in

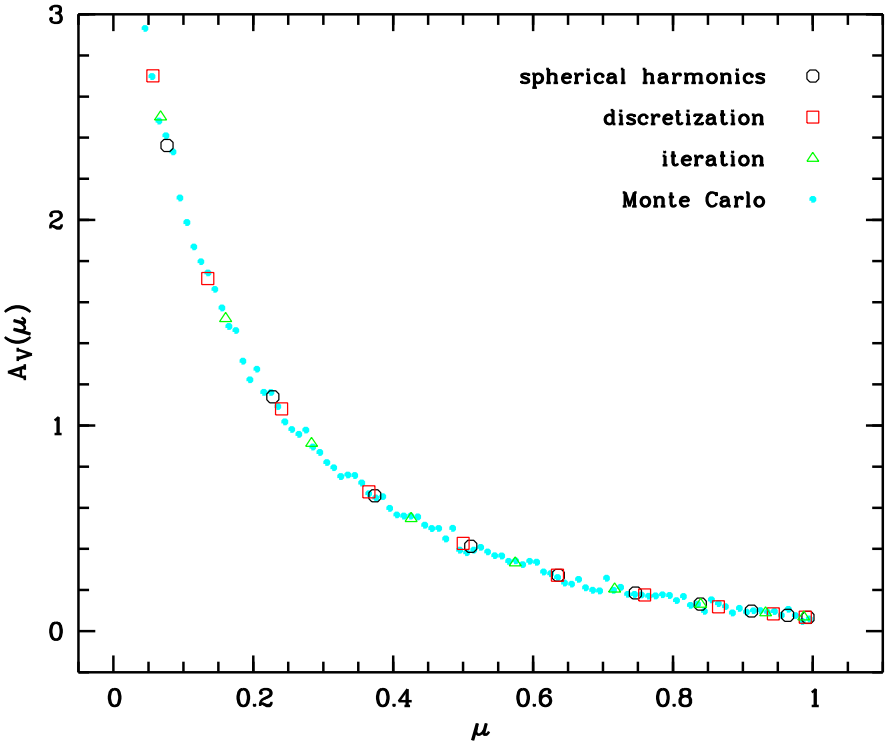

Figure 2. Comparison of the V band attenuation curve $A_V(\mu)$ obtained by the four different methods. The results are only shown for the particular values for which the different methods yield the solution directly (see text).

(i) *the solution method.* In five of the mentioned papers the RTE is solved exactly (i.e. taking absorption and scattering fully into account) using the discretization, iteration or Monte Carlo techniques, whereas Guiderdoni & Rocca-Volmerange (1987) and Calzetti et al. (1994) use approximate analytical solutions.

(ii) *the grain properties.* The fact that different authors use different sets of optical properties can introduce substantial discrepancies in the attenuation curve. These differences between the various values for the grain properties can be very substantial, as clearly shown in Figures 1 and 2 of Di Bartolomeo et al. (1995).

(iii) *the geometry.* As Di Bartolomeo et al. (1995) indicated, it is sometimes impossible to compare results because the geometrical configuration used by the various authors is not always the same. Witt et al. (1992) use a spherical symmetry, Kylafis & Bahcall (1987) and Byun et al. (1994) adopt a axisymmetric galaxy model, whereas the other authors use a plane-parallel homogeneous slab.

In fact in only two of the seven papers, the RTE is solved exactly for a plane-parallel homogeneous slab: Bruzual et al. (1988) by using the discretization technique and Di Bartolomeo et al. (1995) by adopting the expansion in spherical harmonics. However, the authors adopt a different set of optical properties of the dust grains, and the differences $\Delta A(\mu)$ between the attenuation curves can still be due to the first two points mentioned above.

To test to which degree the adopted technique contributes to the differences in the extinction curve, we consider a plane-parallel slab, and solve the RTE *twice* for each of the four methods at our disposal: once with the dust grain parameters of Di Bartolomeo et al. (1995) –the ones we adopt throughout this paper–, and once with those of Bruzual et al. (1988). For a galaxy with total optical depth $\tau_V = 1$, the results are shown in Figure 3 for the U and I bands. We find a very good agreement between the results obtained by Bruzual et al. (1988) and Di Bartolomeo et al. (1995) respectively, and our results with the corresponding dust parameters. This demonstrates that the attenuation differences ΔA are completely due to the differing dust properties, and that the spherical harmonics and iteration methods are reliable.

7.2 Computational efficiency

Besides being accurate, another desirable quality of a solution method is the computational efficiency, as we explained in the introduction.

For the spherical harmonics method the only numerically costly operations are the calculation of the eigenvalues of a matrix of order $L+1$, the inversion of such a matrix, and $L+1$ simple integrations. Given $L \approx 15$ this cost is relatively low. For the discretization method $2N+1$ matrices of the order M need to be inverted, with typical values $M = 12$ and $N = 100$. Because the computation time for the inversion of a matrix of order M is proportional to $M^{2.8}$ (Press et al. 1989), the numerical cost of the discretization method will be considerably higher. The iteration method requires $3M$ cubic spline fits, and $3LM$ integrations along the line-of-sight, with typical values $L = 40$ and $M = 10$. Although the integrands are well-behaved (the product of a smooth source function with an exponential), such that

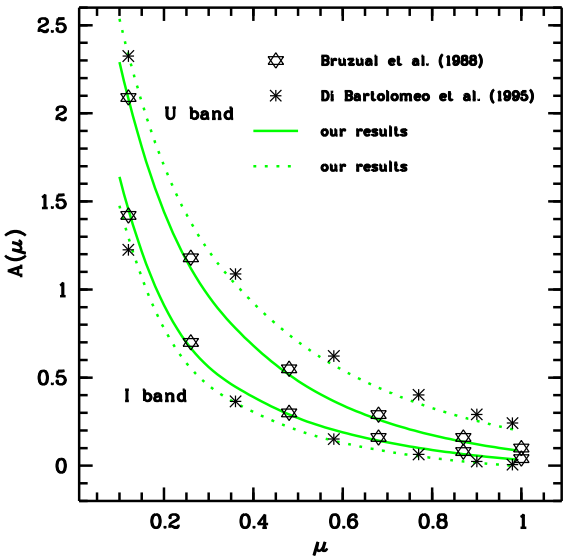

Figure 3. Comparison of our work with that of Bruzual et al. (1988) and Di Bartolomeo et al. (1995). Shown is the attenuation curve for the U and I bands, for a homogeneous slab with $\tau_V = 1$. The stars and asterixes represent the results obtained by Bruzual et al. (1988) and Di Bartolomeo et al. (1995) respectively, the curves are our results where we used the corresponding dust parameters.

Table 3. A comparison of the computation time necessary for the calculation of the attenuation curve $A(\mu)$ for a single wavelength. The number gives the actual computation time in seconds, the second number is the computation time relative to the spherical harmonics method.

spherical harmonics	0.091 s	1
discretization	2.55 s	28
iteration	15.68 s	172
Monte Carlo	15.25 s	168

each individual integration is relatively easy to perform, the high number of integrations makes the iteration method numerically costly. Finally, for the Monte Carlo simulation, the only costly operation for each photon trajectory is the generation of $2n + 3$ pseudo-random numbers, where n is the number of scatterings for the photon. Because the number of photons must be fairly high in order to achieve reliable statistics (we use $N = 10^5$), the numerical cost of the Monte Carlo method is considerable.

In Table 3 we tabulate the mean computation time necessary for the calculation of the attenuation curve for a single wavelength. This little table shows that the iteration method and the Monte Carlo simulation have the same efficiency, and that the spherical harmonics method is significantly more efficient that the other methods. Although for this simple one-dimensional plane-parallel geometry the efficiency is less important (the computation times are very feasible for *all* methods), it will be important if we want to extend these solution to more complex geometries.

7.3 Extension to more complex geometries

The implementations described in this paper can handle the RTE in a plane-parallel geometry, and although they can accomodate any vertical star-dust geometry, they cannot model real disc galaxies. More realistic models require a light distribution that also decreases exponentially in the radial direction (Freeman 1970, Saio & Yoshii 1990, Firmani et al. 1996). Instead of a one-dimensional plane-parallel geometry, the RTE then has to be solved in a two-dimensional axisymmetric geometry, with a set of four independent coordinates instead of a pair. This extra dimension complicates the RTE substantially. This observation forces us to think about how the techniques described in this paper can be generalized to solve the RTE in axisymmetric disc galaxy models.

The most obvious candidate for extension to axisymmetric galaxy models (or any other geometry) is the Monte Carlo simulation. This technique has already been applied several times to realistic disc galaxy models (e.g. Bianchi et al. 1996, Ferrara et al. 1996, de Jong 1996, Wood & Jones 1997, Matthews & Wood 2000). Besides being able to treat any geometry, it is also sufficiently flexible to treat, for example, clumpy dust distributions (Witt & Gordon 1996, 2000, Bianchi et al. 2000). This flexibility makes Monte Carlo simulations probably the most powerful technique for solving complicated radiative transfer problems. However, their great numerical cost is a disadvantage, and this cost will grow strongly if the method is extended to axisymmetric geometries. Indeed, given an initial position, direction and a pathlength, the next position on the path is directly calculated in our plane-parallel geometry, but in axisymmetric geometries this becomes a very time-consuming operation (Bianchi et al. 1996). Therefore it is worth while to investigate how the other techniques can be generalized.

Also the iteration technique is easily extendible to more complex geometries. And in contrast to the Monte Carlo simulation, it can be expected that the numerical cost will grow in proportion to the number of dimensions. If meshes of order J and K are constructed inorder to account for the extra radial and azimuthal dimensions in axisymmetric geometry, the entire routine can be expected to take about JK times as much computation times. The iteration method has been adopted to solve the RTE for axisymmetric disc galaxies in its original form (Vansevičius et al. 1997), but it is the modification by Kylafis & Bahcall (1987) that has increased the efficiency considerably, and turned the method into a very practical instrument to investigate dust attenuation in disc galaxies (Bosma et al. 1992, Byun et al. 1994, Misiriotis et al. 2000). In particular, the method has been adopted to construct detailed radiative transfer models for a set of highly inclined disc galaxies (Xilouris et al. 1997, 1998, 1999), which have been compared with dust emission models (Alton et al. 2000). It is interesting that the results of Xilouris et al. (1999) seem at a first glance not in correspondence with the Monte Carlo results of Kuchinski et al. (1998), whose computed optical depths are approximately a factor 2-3 higher.

In the previous paragraph, it was shown that, while the efficiency of the Monte Carlo and iteration techniques is comparable (at least for the one-dimensional geometry), the spherical harmonics method is superb in efficiency. It is in fact possible to extend the expansion in spherical har-

monics to geometries other than plane-parallel or spherical (Davison 1957). However, another way to extend the spherical harmonics technique to axisymmetric disc galaxies has been proposed by Corradi et al. (1996), who assume a *local* plane-parallel geometry along each line-of-sight. The RTE can then be solved for each line of sight separately, such that the computation time will be very small. The limitation of this method however is that the assumption of a local plane-parallel geometry must remain acceptable. For (nearly) face-on galaxies this may be the case, because the scale at which the galaxy's structure (i.e. the source function) changes on the plane of the sky is small compared to the mean free path of the photons. For highly inclined galaxies however, the mean free path of the photons is large compared to the scale of variation of the source function on the plane of the sky, such that the assumption of local plane-parallel geometry will not be applicable.

The last described method, the discretization method is a typical one-dimensional technique and is least suitable for extension to more complex geometries.

8 CONCLUSION

Constructing radiative transfer models for disc galaxies requires a solution of the RTE. This equation is, even for the most simple geometries, sufficiently complex, such that sophisticated methods are necessary to solve them. The RTE typically takes as input the distribution of stars and dust, and the output is the projected image on the sky. However, usually the problem is the reverse: the distribution of dust and stars has to be derived from the observed intensity. The most simple way to solve this problem is to find a best fitting solution of the RTE in a large parameter space. This involves that the RTE has to be solved repeatedly, such that *efficiency* is a very important property of a good solution method. For the same reason *accuracy* is important: the effects of dust on the attenuation on certain physical parameters can be very weak, such that a high accuracy is required to determine the stellar and dust distribution. And last but not least, there are many ways to solve the RTE for simple one-dimensional geometries, but the modelling of real galaxies demands methods which are applicable to geometries other than plane-parallel or spherical, in the first place axisymmetric. Therefore *flexibility* is necessary.

Several techniques are adopted in the literature to solve the RTE, even for realistic axisymmetric disc galaxy models, but the accuracy, efficiency and flexibility of these methods has never been properly compared. Nevertheless, it is clear that knowledge of these properties is necessary in order to select the most suitable method for a particular radiative transfer problem.

In this paper we investigate four different methods to solve the RTE in a simple plane-parallel geometry: the spherical harmonics method, the discretization method, an iterative method and a Monte Carlo simulation. All of them are adapted such that they solve the RTE exactly (i.e. with the physical processes of absorption and multiple scattering properly taken into account), and that they allow an arbitrary vertical distribution of stars and dust and an arbitrary ARF. This way our methods can contribute to understanding of the transfer of radiation in realistic galactic discs.

For a galaxy model with realistic vertical structure and dust parameters, all four methods yield exactly the same results, with differences between the attenuation curves at most a few hundredths of a magnitude. They can thus be considered as accurate. We also compare our results with those obtained by others, and find that the results are in agreement with each other. Concerning efficiency, the iteration method and Monte Carlo method are close, whereas the discretization method is 6 times as efficient, and the spherical harmonics method even 170 times. Whereas the Monte Carlo method can easily be generalized to an arbitrary geometry, we anticipate that the iteration method will probably be the most efficient routine in axisymmetric geometry. The adaptation of the routine to axial symmetry is more or less straightforward, and the efficiency will not suffer as much from the extra dimensions as the Monte Carlo simulation. This issue will be thoroughly investigated and presented in a forthcoming paper.

REFERENCES

Alton P. B., Xilouris E. M., Bianchi S., Davies J., Kylafis N., 2000, A&A, 356, 795

Baes M., Dejonghe H., 2001a, in *Galaxy Discs and Disc Galaxies*, Funes J. G. and Corsini E. M. eds., ASP Conference Series, in press

Baes M., Dejonghe H., 2001b, submitted to MNRAS

Berlind A. A., Quillen A. C., Pogge R. W., Sellgren J., 1997, AJ, 114, 107

Bianchi S., Ferrara A., Giovanardi C., 1996, ApJ, 465, 127

Bianchi S., Ferrara A., Davies J. I., Alton P. B., 2000, MNRAS, 311, 601

Boselli A., Gavazzi G., 1994, A&A, 283, 12

Bosma A., Byun Y., Freeman K. C., Athanassoula E., 1992, ApJ, 400, L21

Bruzual A. G., Magris C. G., Calvet N., 1988, ApJ, 333, 673

Buat V., Burgarella D., 1998, A&A, 334, 772

Burnstein D., Haynes M., Faber S., 1991, Nature, 353, 515

Byun Y. I., Freeman K. C., Kylafis N. D., 1994, ApJ, 432, 114

Calzetti D., Kinney A. L., Storchi-Bergmann T., 1994, ApJ, 429, 582

Cashwell E. D., Everett C. J., 1959, A Practical Manual on the Monte Carlo Method for random Walk Problems, Pergamon, New York

Chandrasekhar S., 1960, Radiative Transport, Dover Publications, New York

Corradi R. L. M., Beckman J. E., Simonneau E., 1996, MNRAS, 282, 1005

Davies J. I., Burnstein D., 1995, The Opacity of Spiral Disks, Kluwer Academic Publishers, Dordrecht

Davison B., 1957, Neutron Transport Theory, Clarendon Press, Oxford

de Jong R. S., 1996, A&A, 313, 377

Di Bartolomeo A., Barbaro G., Perinotto M., 1995, MNRAS, 277, 1279

Disney M., Davies J., Phillipps S., 1989, MNRAS, 239, 939

Ferrara A., Bianchi S., Dettmar R.-J., Giovanardi C., 1996, ApJS, 123, 437

Firmani C., Hernandez X., Gallagher J., 1996, A&A, 308, 403

Flannery B. P., Roberge W., Rybicki G. B., 1980, ApJ, 236, 598

Freeman K. C., 1970, ApJ, 160, 811

Giovanelli R., Haynes M. P., Salzer J. J., Wegner G., Da Costa L. N., Freudling W., 1994, AJ, 107, 2036

Gradshteyn I. S., Ryzhik I. M., 1965, Table of Integrals, Series and Products, Academic Press Inc., New York

Guiderdoni B., Rocca-Volmerange B., 1987, A&A, 186, 1
James P. A., Puxley P. J., 1993, Nature, 363, 240
Jansen R. A., Knapen J. H., Beckman J. E., Peletier R. F., Hes R., 1994, MNRAS, 270, 373
Henyey L. G., 1937, ApJ, 85, 107
Henyey L. G., Greenstein J. L., 1941, ApJ, 93, 70
Kuchinski L. E., Terndrup D. M., Gordon K. D., Witt A. N., 1998, AJ, 115, 1438
Kylafis N. D., Bahcall J. N., 1987, ApJ, 317, 637
Maccioni A., Perinotto M., 1994, A&A, 284, 241
Matthews L. D., Wood K., 2000, astro-ph/0010033
Mattila K., 1970, A&A, 9, 53
Milkey R. W., Shine R. A., Mihalas D., 1975, ApJ, 217, 425
Misiriotis A., Kylafis N. D., Papamastorakis J., Xilouris E. M., 2000, A&A, 353, 117
Ohta K., Kodaira K., 1995, PASJ, 47, 17
Peletier R. F., Valentijn E. A., Moorwood A. F. M., Freudling W., Knapen J. H., Beckman J. E., 1995, A&A, 300, L1
Pizagno J., Rix H.-W., 1998, AJ, 116, 2191
Pohlen M., Dettmar R.-J., Lütticke R., Schwarzkopf U., 2000, A&AS, 144, 405
Press W. H., Flannery B. P., Teukolsky S. A., Vetterling W. T., 1989, Numerical Recipes, Cambridge University Press, Cambridge
Rönnback J., Shaver P. A., 1997, A&A, 322, 38
Roberge W. G., 1983, ApJ, 275, 292
Saio H., Yoshii Y., 1990, ApJ, 363, 40
Schwarzkopf U., Dettmar R.-J., 2000, A&A, 361, 451
Valentijn E. A., 1990, Nature, 346, 153
Valentijn E. A., 1994, MNRAS, 266, 614
Vansevičius V., Arimoto N., Kodaira K., 1997, ApJ, 474, 623
van de Hulst H. C., de Jong T., 1969, Physica, 41, 151
van der Kruit P. C., Searle L., 1981, A&A, 95, 105
Wainscoat R. J., Freeman K. C., Hyland A. R., 1989, ApJ, 337, 163
White R. E. III, Keel W. C., 1992, Nature, 346, 153
White R. E. III, Keel W. C., Conselice C. J., 2000, ApJ, 542, 761
Witt A. N., 1977, ApJS, 35, 1
Witt A. N., Gordon K. D., 1996, ApJ, 463, 681
Witt A. N., Gordon K. D., 2000, ApJ, 528, 799
Witt A. N., Thronson H. A. Jr., Capuano J. M. Jr., 1992, ApJ, 393, 611
Wood K., Jones T. J., 1997, AJ, 114, 1405
Xilouris E. M., Kylafis N. D., Papamastorakis J., Paleologou E. V., Haerendel G., 1997, A&A, 325, 135
Xilouris E. M., Alton P., Davies J., Kylafis N. D., Papamastorakis J., Trewhella M., 1998, A&A, 331, 894
Xilouris E. M., Byun Y., Kylafis N. D., Paleologou E. V., Papamastorakis J., 1999, A&A, 344, 868
Xu C., Helou G., 1996, ApJ, 456, 163
Yusef-Zadeh F., Morris M., White R. L., 1984, ApJ, 278, 186

APPENDIX A: THE HENYEY-GREENSTEIN ANGULAR REDISTRIBUTION FUNCTION

In general, the phase function $\Phi(\boldsymbol{n},\boldsymbol{n}')$ defines the probability that a photon, that is scattered from a direction $\boldsymbol{n}'$, will obtain a new direction $\boldsymbol{n}$. If we normalize the phase function as

$$\iint \Phi(\boldsymbol{n},\boldsymbol{n}')\frac{\mathrm{d}\boldsymbol{n}'}{4\pi} = 1 \qquad \text{for all } \boldsymbol{n}, \tag{A1}$$

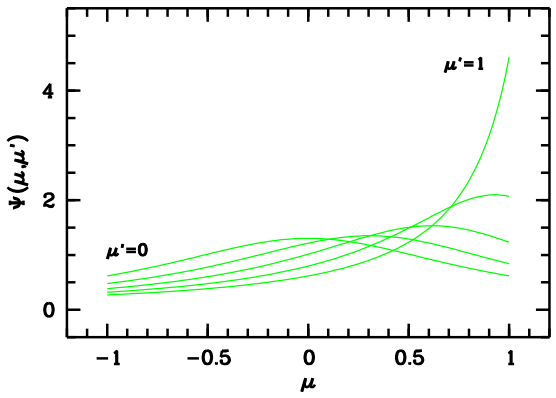

Figure A1. The V band Henyey-Greenstein ARF $\Psi(\mu,\mu')$ as a function of the new direction μ. It is shown for various values of the initial direction μ', ranging between 0 and 1, with intermediate step 0.25. For negative values of μ' the ARF is obtained by the symmetry relation $\Psi(\mu,-\mu') = \Psi(-\mu,\mu')$.

then the amount of photons added to the radiation field $I(\boldsymbol{r},\boldsymbol{n})$ at a position $\boldsymbol{r}$ into a direction $\boldsymbol{n}$ due to scattering is

$$\omega\kappa(\boldsymbol{r}) \iint I(\boldsymbol{r},\boldsymbol{n}')\Phi(\boldsymbol{n},\boldsymbol{n}')\frac{\mathrm{d}\boldsymbol{n}'}{4\pi}. \tag{A2}$$

It can be assumed that the scattering phase function does not depend independently on the four variables $(\boldsymbol{n},\boldsymbol{n}') = (\mu,\phi,\mu',\phi')$. We assume that it depends on them only through the angle Θ between the incident and the scattered radiation. In our plane-parallel geometry, we have azimuthal symmetry, and the scattering term can then be written as

$$\frac{1}{2}\omega\kappa(z)\int_{-1}^{1} I(z,\mu')\Psi(\mu,\mu')\mathrm{d}\mu', \tag{A3}$$

where the ARF $\Psi(\mu,\mu')$ is defined as (van de Hulst & de Jong 1969, Bruzual et al. 1988)

$$\Psi(\mu,\mu') = \frac{1}{2\pi}\int_0^{2\pi} \Phi(\cos\Theta)\mathrm{d}\phi'. \tag{A4}$$

A widely used phase function is the one named after Henyey and Greenstein (1941),

$$\Phi(\cos\Theta) = \frac{1-g^2}{(1+g^2-2g\cos\Theta)^{3/2}}, \tag{A5}$$

which is an accurate one-parameter family to describe the average scattering in galactic dust. Its parameter g is the asymmetry parameter and is the mean cosine of the scattering angle, $g = \langle\cos\Theta\rangle$. A very useful characteristic of this function is that it has a very simple expansion in Legendre polynomials. Using the generating function for Legendre polynomials it is easily shown that

$$\Phi(\cos\Theta) = \sum_{l=0}^{\infty}(2l+1)g^l P_l(\cos\Theta), \tag{A6}$$

such that we immediately have an expression for the angular redistribution function (Chandrasekhar 1960, Roberge 1983)

$$\Psi(\mu,\mu') = \sum_{l=0}^{\infty}(2l+1)g^l P_l(\mu)P_l(\mu'). \tag{A7}$$

In order to derive a closed expression for $\Psi(\mu,\mu')$ we use

$$\cos\Theta = \mu\mu' + \sqrt{(1-\mu^2)(1-\mu'^2)}\cos(\phi-\phi'). \tag{A8}$$

and combine this expression with (A4) and (A5), to obtain

$$\Psi(\mu,\mu') = \frac{1-g^2}{\pi}\int_0^\pi \frac{\mathrm{d}t}{(a\pm b\cos t)^{3/2}} \tag{A9}$$

with

$$a(\mu,\mu') = 1+g^2-2g\mu\mu' \tag{A10}$$

$$b(\mu,\mu') = 2|g|\sqrt{(1-\mu^2)(1-\mu'^2)} \tag{A11}$$

For all values of the asymmetry parameter, these functions obey the relation $a > b \geqslant 0$ such that we find (Gradshteyn & Ryzhik, 1965, Section 2.575)

$$\Psi(\mu,\mu') = \frac{2(1-g^2)}{\pi(a-b)\sqrt{a+b}}E\left(\sqrt{\frac{2b}{a+b}}\right), \tag{A12}$$

where $E(k)$ is the complete elliptic integral of the second kind. Figure A1 shows the Henyey-Greenstein ARF at the V band for a few values of the initial direction μ'.

This paper has been produced using the Royal Astronomical Society/Blackwell Science LaTeX style file.